1034 J. Am. Chem. Soc. **1990**, *112*, 1034-1038

Electron-Transfer Kinetics of Contacting Monolayers

J. C. Jernigan and Royce W. Murray*

Contribution from the Kenan Laboratories of Chemistry, University of North Carolina, Chapel Hill, North Carolina 27599-3290. *Received June 15, 1989*

Abstract: The rates of electron-transfer reactions between the monolayers of metal complexes in contact at polymer/polymer interfaces have been evaluated for the thermodynamically disfavored cross-reactions poly[Os(bpy)$_2$(vpy)Cl]$^{2+}$ + poly[Os(bpy)$_2$(vpy)$_2$]$^{2+}$, poly[Os(bpy)$_2$(vpy)$_2$]$^{3+}$ + poly[Ru(vbpy)$_3$]$^{2+}$, and poly[Os(bpy)$_2$(vpy)$_2$]$^{3+}$ + poly[Ru(bpy)$_2$(vpy)$_2$]$^{2+}$. An analysis of the interfacial electron-transfer rates that accounts for the thermodynamically favored back-reaction gives rate constants 2.8 × 10^3, 1.1 × 10^3, and 2 × 10^2 M^{-1} s^{-1}, respectively, that agree with values estimated from classical electron-transfer theory: 3.1 × 10^3, 1.1 × 10^3, and 1.5 × 10^2 M^{-1} s^{-1}. The second of these three reactions was studied with the two polymer films both in contact and separated by a metal junction, with no discernable difference in the results. The metal-separated experiment allowed examination of the polymer/polymer junction's interfacial potential, which is interpreted as a mixed potential.

In the substantial literature on the kinetics of electron-transfer reactions, the dynamics of electron transfers across contacting interfaces of rigid media remain a largely unexplored area. We have reported previously[1] on this topic, in an experiment in which ultrathin polymer films composed of two different metal complexes, poly[Ru(vbpy)$_3$](ClO$_4$)$_2$ and poly[Os(bpy)$_2$(vpy)$_2$](ClO$_4$)$_2$, were electrochemically grown in contact. The rate of interfacial electron transfers for the thermodynamically disfavored (by 0.40 V) cross-reaction between the monolayers of metal complexes in contact at the polymer/polymer interface was estimated with an

$$\text{poly[Ru(vbpy)}_3]^{2+} + \text{poly[Os(bpy)}_2\text{(vpy)}_2]^{3+} \rightarrow \text{poly[Ru(vbpy)}_3]^{3+} + \text{poly[Os(bpy)}_2\text{(vpy)}_2]^{2+} \quad (1)$$

electrochemical procedure as about 5 × 10^{-9} mol/(cm^2·s), corresponding to a rate constant for reaction 1 of 32 M^{-1} s^{-1}. This was the first description of the rate of a redox reaction between contacting monomolecular layers of different metal complexes. The kinetic result was striking because the rate constant obtained was only about 30× smaller than a prediction based on classical electron-transfer theory[2] and analogy with reactions of the monomer complexes in fluid solutions.[3]

The present report is a further study of reaction 1 and of two similar interfacial reactions, shown schematically in Figure 1. Note that reaction 2 is the same as (the previously studied) reaction 1 except that in the new experiment the two reacting polymer films are not in direct contact but are separated by a metal layer. This allowed inspection of possible factors relating to how the polymer film is contacted and also allowed a direct measurement of the potential of the polymer–polymer interface. Reactions 3 and 4 are newly reported interfacial processes, which we investigated in the interest of evaluating the free energy dependence of the reaction rate. Reactions 3 and 4 are studied as metal film separated and directly contacting polymer interfaces, respectively.

All of the reactions in Figure 1 occur in the *thermodynamically disfavored* electron-transfer direction. Like our work with polymer film/solution interfaces,[4] this was done in order that the electron transfers between metal complex sites at the polymer/polymer interfaces be much slower than the self-exchange (electron hopping) reactions between metal complex sites that occur within the two polymer films as the mechanism of transporting electrons to and from the polymer/polymer interface. The interfacial reactions are driven in the thermodynamically disfavored direction by manipulating the potentials of metal electrodes contacting the opposite faces of the polymer films, and the rates of the interfacial electron transfers are measured as currents flowing through the electrodes.

The results show that the rate of all the electron-transfer reactions in Figure 1, including the previously studied[1] reaction 1, are quantitatively consistent with predictions from classical electron-transfer rate theory,[2] provided the electron-transfer back-reactions (which in our experiment are in the thermodynamically favored reaction direction) are accounted for in the data analysis.

Experimental Section

Chemicals and Equipment. The metal complex monomers used for Figure 1 were synthesized as reported previously.[5] Acetonitrile solvent (Burdick and Jackson, Spectroquality) was stored over 4A molecular sieves. The electrochemical instrument was a Pine Instruments Model RDE4 with which potentials of two working electrodes could be independently controlled vs a SSCE (NaCl saturated calomel electrode) reference electrode.

Electrochemical Measurements. Electrochemical polymerizations were done as previously described,[5] using 0.5 mM [Os(bpy)$_2$(vpy)$_2$](PF$_6$)$_2$ and [Ru(bpy)$_2$(vpy)$_2$](PF$_6$)$_2$, 2 mM [Os(bpy)$_2$(vpy)Cl](PF$_6$), and 0.25 mM [Ru(vbpy)$_3$](PF$_6$)$_2$ monomer solutions in degassed 0.1 M Et$_4$NClO$_4$/CH$_3$CN. The Pt electrode potential was swept repeatedly between −1.0 and −1.65 V vs. SSCE until a polymer film containing about 10^{-8} mol/cm^2 of metal complex sites had accumulated on the electrode. In the studies of reactions 1 and 4, a second polymer film was grown on top of the first polymer; it was then overcoated with a thin, porous evaporated Au electrode[6] to make a metal/polymer/polymer/metal sandwich. In the case of reactions 2 and 3, two Pt/polymer/Au sandwiches (each containing a single polymer) were contacted serially by the Pt electrodes.

In all polymer/polymer rate measurements, the metal/polymer/polymer/metal sandwiches and metal/polymer/metal/polymer/metal serial sandwiches were immersed in 0.1 M Et$_4$ClO$_4$/CH$_3$CN electrolyte solution containing Pt wire auxiliary and SSCE or Ag wire reference electrode. The electrolyte solution provides the counterions required, for electroneutrality, to drive one of the two polymers into the oxidized state. In the interfacial kinetics experiment, the potential of one of the two outer metal contacts of the Pt/polymer/polymer/Au and Au/polymer/Pt–Pt/polymer/Au sandwiches was typically held at a fixed value (E_{fixed} vs SSCE) and the other scanned positively (E_{scan} vs SSCE). The currents at each electrode could be independently measured.

Results and Discussion

The interfacial electron-transfer experiment requires that electrons be delivered to and from the polymer interfaces solely by the electron self-exchange reactions of the principal metal complex redox couples of the polymer (Figure 1). The presence of impurity couples in the polymers that might cause electron transport through the polymers at potentials different from those of the principal redox reactants would alter the effective interfacial reaction free energy and invalidate the kinetic measurements. The cyclic voltammetry of electropolymerized films of the four metal polypyridine polymers employed (Figure 2) is well defined. Alternative electron-transport paths, which would be indicated in the voltammetry by the presence of additional reversible current peaks, appear to be absent.

---

(1) Leidner, C. R.; Murray, R. W. *J. Am. Chem. Soc.* **1985**, *107*, 551.
(2) Marcus, R. A. *Annu. Rev. Phys. Chem.* **1964**, *15*, 155.
(3) Chan, M.; Wahl, A. C. *J. Phys. Chem.* **1978**, *82*, 2542.
(4) Leidner, C. R.; Murray, R. W. *J. Am. Chem. Soc.* **1984**, *106*, 1606.
(5) Denisevich, P.; Abruna, H. D.; Leidner, C. R.; Meyer, T. J.; Murray, R. W. *Inorg. Chem.* **1982**, *21*, 2153.
(6) Jernigan, J. C.; Murray, R. W. *J. Am. Chem. Soc.* **1987**, *109*, 1738.

0002-7863/90/1512-1034$02.50/0

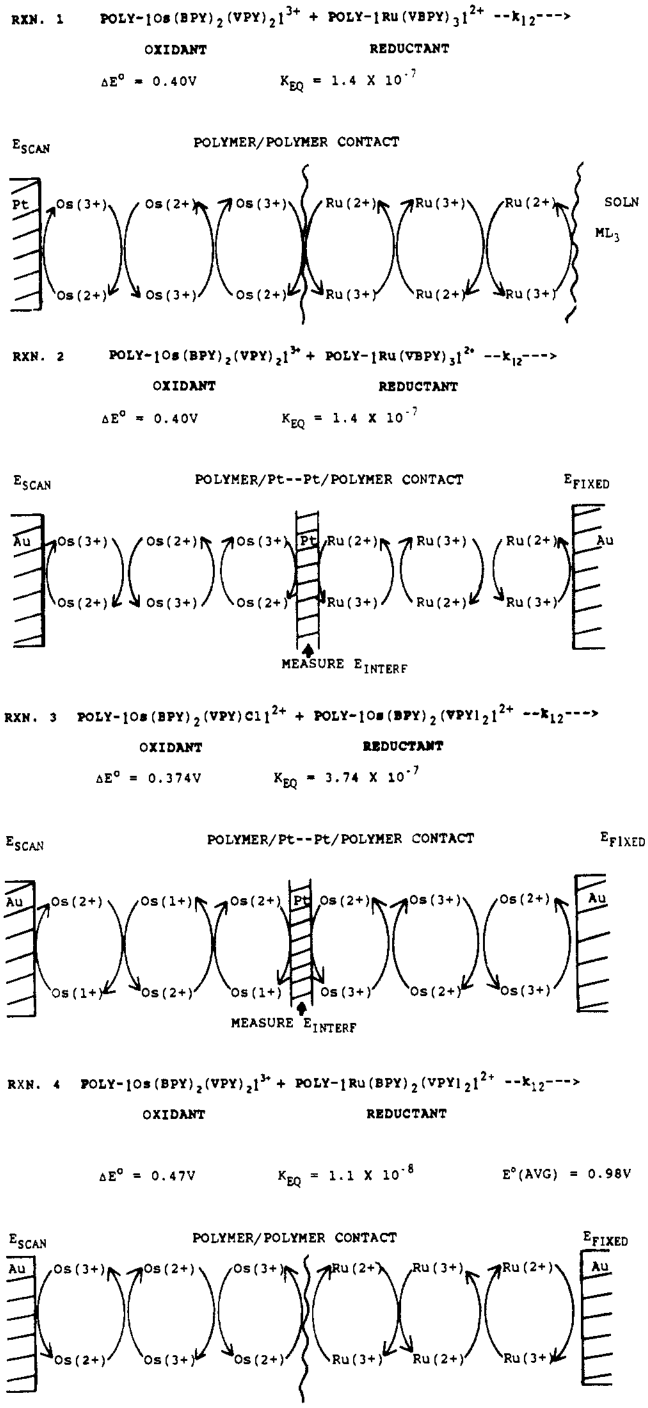

Figure 1. Schematic diagrams of four interfacial reactions studied. The individual formal potentials are poly$[Ru(bpy)_2(vpy)_2]^{3+/2+}$, $E°$ = 1.21 V vs SSCE; poly$[Ru(vbpy)_3]^{3+/2+}$, $E°$ = 1.14 V vs SSCE; poly$[Os(bpy)_2(vpy)_2]^{3+/2+}$, $E°$ = 0.74 V vs SSCE; and poly$[Os(bpy)_2(vpy)Cl]^{2+/1+}$, $E°$ = 0.37 V vs SSCE.

Current-potential curves are shown in Figure 3 for four different pairs (curves B-D are the pairs in reactions 2-4 in Figure 1) of contacting (directly or as serial sandwiches) polymer films. The curves were taken by holding the potential of the electrode contacting the polymer that acts as reductant in the interfacial reaction at a negative value (E_{fixed}), to maintain it in a reduced state. The potential (E_{scan}) of the electrode contacting the polymer that is to be the interfacial oxidant is then scanned (vs an SSCE in the solution) toward positive values. The currents shown are those measured at the reducing electrode.

Curve A in Figure 3 corresponds to the case where two *identical* polymer films are contacted as serial Au/polymer/Pt-Pt/polymer/Au sandwiches; this situation is not shown in Figure 1. In this case, when potentials are applied to the external electrodes so as to oxidize poly$[Os(bpy)_2(vpy)_2]^{2+}$ at one electrode and to reduce poly$[Os(bpy)_2(vpy)_2]^{3+}$ at the other, the reaction at the polymer/Pt/polymer interface is a self-exchange reaction and is

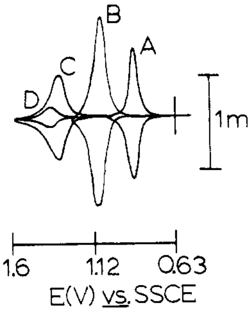

Figure 2. Cyclic voltammetry at 0.05 V/s in 0.1 M Et_4ClO_4/CH_3CN of (curve A) poly$[Os(bpy)_2(vpy)Cl]^{2+/1+}$ ($\Gamma_{TOTAL} = 1.5 \times 10^{-8}$ mol/cm^2), (curve B) poly$[Os(bpy)_2(vpy)_2]^{3+/2+}$ ($\Gamma_{TOTAL} = 2.3 \times 10^{-8}$ mol/cm^2), (curve C) poly$[Ru(vbpy)_3]^{3+/2+}$ ($\Gamma_{TOTAL} = 1.4 \times 10^{-8}$ mol/cm^2), and (curve D) poly$[Ru(bpy)_2(vpy)_2]^{3+/2+}$ ($\Gamma_{TOTAL} = 0.46 \times 10^{-8}$ mol/cm^2) films on Pt electrodes.

$$\text{poly}[Os(bpy)_2(vpy)_2]^{3+} + \text{poly}[Os(bpy)_2(vpy)_2]^{2+} \rightarrow \text{poly}[Os(bpy)_2(vpy)_2]^{2+} + \text{poly}[Os(bpy)_2(vpy)_2]^{3+} \quad (5)$$

identical with the self-exchange reactions occurring as a means of electron transport within the bulk of the two films. The current that flows through this pair of films is, within experimental uncertainty, the same as that which would be measured in a single Pt/polymer/Au sandwich of the same polymer, with an overall polymer thickness equal to the sum of the two films in curve A. The current in curve A is therefore simply controlled by the rate of electron self exchange between identical polymer sites. This experiment serves to demonstrate that, within experimental uncertainty (vide infra), the presence of the polymer/Pt-Pt/polymer junction in reactions 2, 3, and 5, in and of itself, causes no significant impediment to current flow.

The current-potential curves C, B, and D in Figure 3 correspond to the thermodynamically disfavored reactions 2, 3, and 4, respectively, occurring at the interfaces between the three pairs of polymers. At potentials that produce limiting currents (i_{lim}) on the curves, the polymer/polymer interfacial reactions are being driven at maximal rates. At these potentials, one polymer film is controlled by its contacting electrode to be in the nearly all-reduced state, while the other is in the nearly all-oxidized state. Table I exhibits the limiting currents for reactions 2, 3, and 4, expressed as interfacial reaction rates (i_{lim}/nFA, mol/(cm^2·s)), for the three polymer pairs in a series of experiments. The interfacial electron transfer kinetic constants will be derived from these results (vide infra).

There are additional noteworthy aspects of Figure 3. First, from the data given at the top of the figure, a comparison of the current sensitivities (S) in Figure 3 to the differences in formal potentials of the polymer redox couples ($\Delta E°$) shows that the rates of the polymer/polymer reactions *decrease systematically as the interfacial reaction becomes more thermodynamically disfavored.* Thus, the limiting current for reaction 2 (curve C) is less than that of the less disfavored reaction 3 (curve B). This effect was hoped for as it shows that the interfacial reaction rate is responsive to the free energy difference. No current could be measured at all across the interface between another pair of polymers, poly$[Os(bpy)_2(vpy)_2]^{3+}$/Pt/poly$[Ru(4\text{-}Cl\text{-}phen)_2(vpy)_2]^{2+}$, which had a difference in polymer formal potential, $\Delta E°$ = 0.55 V, much larger than any in Figure 3. Second, the currents for all of the disfavored reactions (curves B-D) are much less than that for the more nearly isoenergetic curve A (reaction 5). Third, we have found that[7] the rates of electron transport (i.e., reactions like reaction 5) in polymers like those used here are fairly similar to

---

(7) Leidner, C. R.; Schmehl, R. H.; Pickup, P. G.; Murray, R. W. *Proceed. Electrochem. Soc.*; Symposium on Chemical Physics and Electrocatalysis; Electrochemical Society: Pennington, NJ, 1984; p 389.

(8) Pickup, P. G.; Leidner, C. R.; Denisevich, P.; Murray, R. W. *J. Electroanal. Chem.* **1984**, *164*, 39.

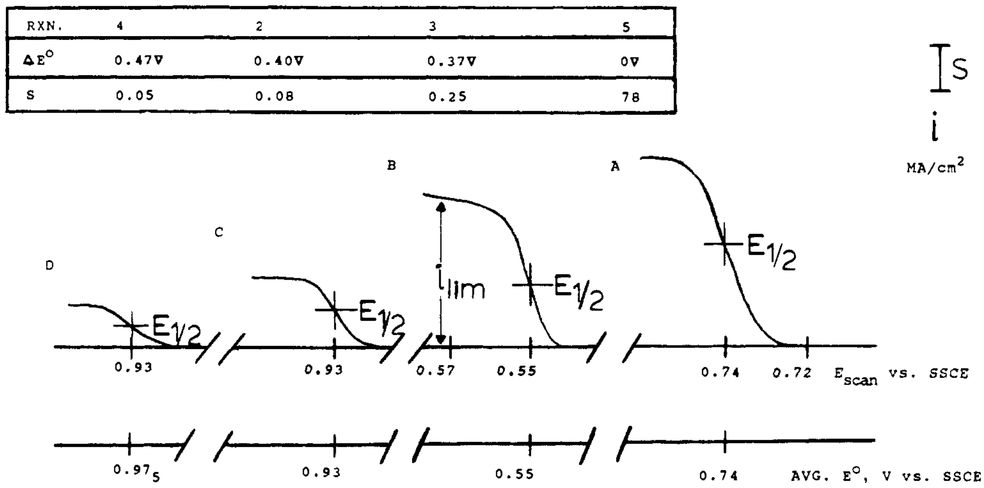

Figure 3. Currents measured at the E_{fixed} electrode as the potential E_{scan} of the other electrode is scanned in a positive (oxidizing) direction, for the following polymer pairs: curve A, Au/poly[Os(bpy)$_2$(vpy)$_2$]$^{3+}$/Pt-Pt/poly[Os(bpy)$_2$(vpy)$_2$]$^{2+}$/Au; curve B, Au/poly[Os(bpy)$_2$(vpy)Cl]$^{2+}$/Pt-Pt/poly[Os(bpy)$_2$(vpy)$_2$]$^{2+}$/Au; curve C, Au/poly[Os(bpy)$_2$(vpy)$_2$]$^{3+}$/Pt-Pt/poly[Ru(vbpy)$_3$]$^{2+}$/Au; and curve D, Au/poly[Os(bpy)$_2$(vpy)$_2$]$^{3+}$/poly[Ru(bpy)$_2$(vpy)$_2$]$^{2+}$/Pt. The polymer pairs are immersed in 0.1 M Et_4ClO_4/CH_3CN electrolyte solution containing an SSCE reference electrode. The numbers shown on the E_{scan} axis of the figure are the half-wave potentials of the waves, and the current sensitivities, S, in mA/cm^2, are the numbers in the box.

Table I. Interfacial Electron-Transfer Rate Data and Fits to Theory for Reactions in Figure 1

Γ, ×10^8 mol/cm^2		intf rate, × 10^9 mol/(cm^2·s)	k_{12}, M^{-1} s^{-1} (assuming k_{21} = 0) eq 6	k_{12}, M^{-1} s^{-1} from eq 9	k_{21}, M^{-1} s^{-1} from eq 9	$k_{12(\text{TH})}$, M^{-1} s^{-1} from eq 7, 8	X^a
Γ_{ox}	Γ_{red}	i_{lim}/nFA					
Reaction 1. Polymer/Polymer Interface poly[Os(bpy)$_2$(vpy)$_2$]$^{3+}$/poly[Ru(vbpy)$_3$]$^{2+}$ → poly[Os(bpy)$_2$(vpy)$_2$]$^{2+}$/poly[Ru(vbpy)$_3$]$^{3+}$ $\Delta E°$ = 0.40 V, K_{EQ} = 1.4 × 10^{-7}							
4.61	1.48	4.7	33	2.0 × 10^3	1.2 × 10^{10}		0.32
2.73	1.96	5.2	37	2.3 × 10^3	1.3 × 10^{10}		0.29
7.04	2.67	4.2	29	1.8 × 10^3	1.0 × 10^{10}		0.36
5.08	2.98	4.1	28	1.7 × 10^3	1.0 × 10^{10}		0.37
				av 2.0 ± 0.2 × 10^3	1.1 × 10^{10}	0.9 × 10^3	
Reaction 2. Polymer/Pt-Pt/Polymer Interface poly[Os(bpy)$_2$(vpy)$_2$]$^{3+}$/Pt/poly[Ru(vbpy)$_3$]$^{2+}$ → poly[Os(bpy)$_2$(vpy)$_2$]$^{2+}$/Pt/poly[Ru(vbpy)$_3$]$^{3+}$ $\Delta E°$ = 0.40 V, K_{EQ} = 1.4 × 10^{-7}, av $E°$ = 0.94 V vs SSCE, $E_{1/2}$ = 0.93 V vs. SSCE							
1.74	1.4	2.8	20	1.1 × 10^3	6.6 × 10^9		0.51
1.7	1.27	0.9	7	0.6 × 10^3	6.3 × 10^9		0.57
1.64	0.61	2.7	19	1.5 × 10^3	5.9 × 10^9		0.51
				av 1.1 × ±0.3 10^3	6.3 ± 0.2 × 10^9	1.09 × 10^3	
Reaction 3. Polymer/Pt-Pt/Polymer Interface Poly[Os(bpy)$_2$(vpy)Cl]$^{2+}$/Pt/poly[Os(bpy)$_2$(vpy)$_2$]$^{2+}$ → poly[Os(bpy)$_2$(vpy)Cl]$^{1+}$/Pt/poly[Os(bpy)$_2$(vpy)$_2$]$^{3+}$ $\Delta E°$ = 0.37 V, K_{EQ} = 3.74 × 10^{-7}, av $E°$ = 0.55 V vs SSCE, $E_{1/2}$ = 0.55 V vs SSCE							
0.58	1.2	7.6	53	3.5 × 10^3	9.6 × 10^9		0.47
0.75	0.81	2.5	18	1.3 × 10^3	2.3 × 10^9		0.95
0.60	1.24	6.9	49	3.7 × 10^3	1.0 × 10^{10}		0.45
		5.3	37	2.5 × 10^3	6.9 × 10^9		0.59
			av 39 ± 16	2.8 ± 0.8 × 10^3	7.2 × 10^9	3.1 × 10^3	
Reaction 4. Polymer/Polymer Interface Poly[Os(bpy)$_2$(vpy)$_2$]$^{3+}$/poly[Ru(bpy)$_2$(vpy)$_2$]$^{2+}$ → poly[Os(bpy)$_2$(vpy)$_2$]$^{2+}$/Pt/poly[Ru(bpy)$_2$(vpy)$_2$]$^{3+}$ $\Delta E°$ = 0.47 V, K_{EQ} = 1.1 × 10^{-8}, av $E°$ = 0.975 V vs SSCE, $E_{1/2}$ = 0.93 V vs SSCE							
2.85	3.4	0.57	4	200	1.5 × 10^{10}		0.48
4.1	4.6	0.52	4	n.a.	n.a.		n.a.
4.2	3.4	0.21	2	n.a.	n.a.		n.a.
2.9	3.4	0.49	4	n.a.	n.a.		n.a.
			av 3 ± 1	200	1.8 × 10^{10}	150	

[a] The values of X for reactions 1–4 correspond to Z values of 1.2 × 10^{11}, 4.9 × 10^{11}, 4 × 10^{11}, and 7 × 10^{11} M^{-1} s^{-1}, respectively.

one another. The reason that the limiting currents for curves B–D are much smaller than that in curve A is therefore attributed to the slowness of the interfacial polymer–polymer reactions as opposed to kinetic electron transport limitations within the polymer films themselves. Fourth, we see from the interfacial rate results (i_{lim}/nFA) in Table I that the rates of reactions 1 and 2 are quite similar, which is consistent with our preceding observation about curve A that the Pt layer between the two polymers in reaction 2 does not, within experimental uncertainty, pose an additional barrier to current flow.

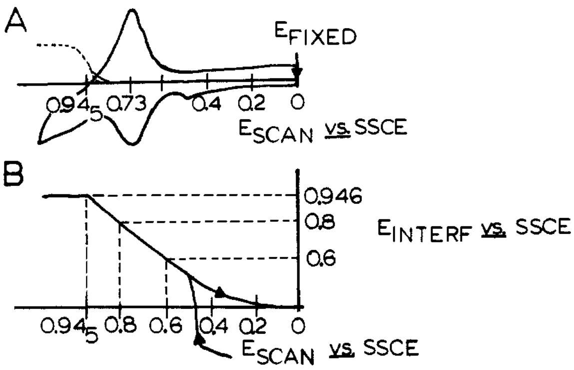

Figure 4. Upper: Currents measured at the E_{fixed} (---) and E_{scan} (—) electrodes for the polymer pair Au/poly$[Os(bpy)_2(vpy)_2]^{3+}$/Pt–Pt/poly$[Ru(vbpy)_3]^{2+}$/Au in 0.1 M Et_4NClO_4/CH_3CN. Lower: The potential of the central Pt layer between the polymer pair vs the potential of the E_{scan} electrode.

Figure 4A displays a more detailed electron-transfer experiment on the polymer pair of reaction 2. Figure 4A shows the currents flowing at both contacting electrodes as the potential of the (Au) electrode contacting the poly$[Os(bpy)_2(vpy)_2]^{2+}$ film is scanned (E_{scan}, Figure 1, reaction 2) to more oxidizing potentials while that on the poly$[Ru(vbpy)_3]^{2+}$ side is maintained at a reducing value (E_{fixed}, Figure 1, reaction 2). The current at the fixed potential electrode (dashed line) lacks interfering processes and most clearly represents the onset of the interfacial reaction 2. Curves B–D in Figure 3 and the interfacial rate data in Table I were derived from results like this. The current at the scanned-potential electrode (solid line) also shows the interfacial wave, but much less clearly owing to the interferences from the concurrent double layer capacitance currents at the potential-scanned, porous Au electrode, and the current peak centered at 0.73 V vs SSCE representing conversion of the poly$[Os(bpy)_2(vpy)_2]^{2+}$ film to its Os(III) state.

Part B of Figure 4 will be considered later.

Turning to the interfacial rates (i_{lim}/nFA in Table I), our previous[1] interfacial rate analysis (of reaction 1) represented the rate as the second-order expression

$$i_{\text{lim}}/\text{nFA} = 10^3 k_{12} \Gamma_{\text{Os(III)}} \Gamma_{\text{Ru(II)}} / \delta \qquad (6)$$

where $\Gamma_{\text{Os(III)}}$ and $\Gamma_{\text{Ru(II)}}$ are the interfacial concentrations of the indicated metal complex sites (mol/cm²) that are in contact at the interface, k_{12} is the second-order cross-electron-transfer rate constant at the polymer/polymer interface (cm³/(mol·s)), and is the site–site spacing and serves to express the interfacial rate constant in homogeneous rate constant units.[6] Values of k_{12} for reactions 1–4, derived from the interfacial rates with eq 6 and taking monolayer values $\Gamma_{\text{Os(III)}} = \Gamma_{\text{Ru(II)}} = 1 \times 10^{-10}$ mol/cm² and $\delta = 1.4$ nm, are given in Table I under the heading "assuming $k_{21} = 0$".

The theoretical value for k_{12} of these reactions can be derived from the classical electron-transfer theory due to Marcus,[2] written as[4]

$$\log k_{12} = 0.5 \log (k_{11} k_{22}) - 8.47 \Delta E^\circ (1 + X \Delta E^\circ) \qquad (7)$$

where

$$X = [0.236 \log (k_{11} k_{22} / Z^2 K^2)]^{-1} \qquad (8)$$

and k_{11} and k_{22} are the electron self-exchange rate constants for electron transfers between the metal complex sites of the two polymers, ΔE° is the difference between their formal potentials and measures the reaction free energy, Z is the collision frequency in M⁻¹ s⁻¹, and K corrects for nonadiabatic effects as noted by Sutin.[9] Calculations of k_{12} from eq 7 and 8, assuming $Z = 10^{11}$ M⁻¹ s⁻¹, $K = 1$, and the monomer complex $[Os(bpy)_3]^{2+}$ and $[Ru(bpy)_3]^{2+}$ literature values[3] $k_{11} = 2.2 \times 10^7$ and 8.3×10^6 M⁻¹ s⁻¹ for the polymer self-exchange rates, gives the $k_{12(\text{TH})}$ values shown in Table I.

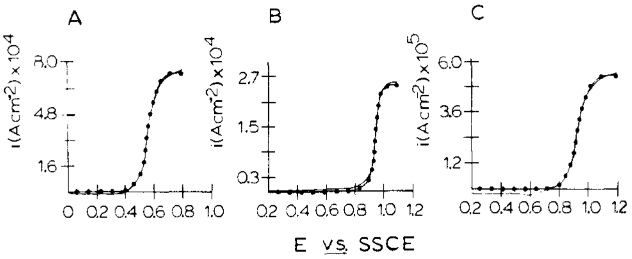

Figure 5. Experimental curve for current due to the interfacial electron-transfer reaction vs E_{scan}, compared to curves calculated from eq 9–12, in which the polymer pairs are the following: panel A, Au/poly$[Os(bpy)_2(vpy)Cl]^{2+}$/Pt–Pt/poly$[Os(bpy)_2(vpy)_2]^{2+}$/Au; panel B, Au/poly$[Os(bpy)_2(vpy)_2]^{3+}$/Pt–Pt/poly$[Ru(vbpy)_3]^{2+}$/Au; and panel C, Au/poly$[Os(bpy)_2(vpy)_2]^{3+}$/poly$[Ru(bpy)_2(vpy)_2]^{2+}$/Pt. The parameters used for calculating the theoretical curves are the k_{11} and k_{22} cited in the text, the ΔE° in Figure 1, and the following: panel A, $k_{12} = 3.5 \times 10^3$ M⁻¹ s⁻¹, $k_{21} = 9.6 \times 10^9$ M⁻¹ s⁻¹, $X = 0.47$; panel B, $k_{12} = 1.1 \times 10^3$ M⁻¹ s⁻¹, $k_{21} = 6.6 \times 10^9$ M⁻¹ s⁻¹, $X = 0.51$; panel C, $k_{12} = 200$ M⁻¹ s⁻¹, $k_{21} = 1.5 \times 10^{10}$ M⁻¹ s⁻¹, $X = 0.48$.

It is obvious that the k_{12} values evaluated from eq 6 are smaller than the $k_{12(\text{TH})}$ results by 50–70×. We observed this difference in our previous study[1] of reaction 1, where we speculated about several possible non-idealities in the nature of the polymer/polymer interface as causing decrease of k_{12}.

We now believe that this discrepancy is due to neglect of the rate of the (thermodynamically favored) back-reactions of reactions 1–4. That is, in reference to reactions 1 and 2, only tiny concentrations of poly$[Os(bpy)_2(vpy)_2]^{2+}$ and poly$[Ru(vbpy)_3]^{3+}$ sites are expected within the polymers over the range of interfacial potentials where the reactions occur. On the other hand, even these tiny concentrations, when combined with a very large back-reaction rate (k_{21}), may have a significant effect on the net reaction rate. We accordingly reformulate eq 6 as

$$i_{\text{lim}}/nFA = 10^3 k_{12} \Gamma_{\text{Os(III)}} \Gamma_{\text{Ru(II)}} / \delta - 10^3 k_{21} \Gamma_{\text{Os(II)}} \Gamma_{\text{Ru(III)}} / \delta \qquad (9)$$

In eq 9, $\Gamma_{\text{Os(III)}}$ and $\Gamma_{\text{Ru(II)}}$ can be taken as nearly equal to $\Gamma_{\text{monolayer}} = 10^{-10}$ mol/cm², but an assumption is necessary to express values of $\Gamma_{\text{Os(II)}}$ and $\Gamma_{\text{Ru(III)}}$. We assume that the rates of reactions 1 and 2 are sufficiently slow, in comparison to electron hopping delivery of poly$[Os(bpy)_2(vpy)_2]^{3+}$ and poly$[Ru(vbpy)_3]^{2+}$ to the interface and removal of poly$[Os(bpy)_2(vpy)_2]^{2+}$ and poly$[Ru(vbpy)_3]^{3+}$ through the polymer films, that interfacial concentrations of these states can be expressed with the Nernst equation, i.e.

$$E = E_{\text{Os}}{}^\circ - (RT/nF) \ln \Gamma_{\text{Os(II)}} / \Gamma_{\text{Os(III)}} = E_{\text{Ru}}{}^\circ - (RT/nF) \ln \Gamma_{\text{Ru(II)}} / \Gamma_{\text{Ru(III)}} \qquad (10)$$

Combining eq 9 and 10, remembering that

$$k_{12}/k_{21} = K_{\text{eq}} = \exp[(RT/nF)(E_{\text{Os}}{}^\circ - E_{\text{Ru}}{}^\circ)] \qquad (11)$$

and using the current–potential form for the interfacial wave

$$E = E_{1/2} + 0.059 \log [(i_{\text{lim}} - i)/i] \qquad (12)$$

we conducted a comparison of theory to the current–potential waves of Figure 3 (curves B–D) by nonlinear least-squares fitting. i_{lim}, k_{11}, k_{22}, $E_{1/2}$, and $E_{\text{Os}}{}^\circ - E_{\text{Ru}}{}^\circ$ were taken as knowns, and k_{12} and (arbitrarily) Z as adjustable parameters.

The results of the preceding analyses are shown in Figure 5, and in Table I in the k_{12} and k_{21} labeled columns labeled "from eq 9". The comparisons in Figure 5 reveal that the shapes of the current–potential curves are well represented by the above relations. This is important in that it reveals that the reaction rate varies in a manner expected for the change in population of $\Gamma_{\text{Os(III)}}$ sites with E_{scan} electrode potential. More significantly, we see that the evaluated (eq 9) k_{12} rate constants are larger than those obtained with eq 6, and now in fact agree quite well with the theoretical $k_{12(\text{TH})}$ values calculated from the classical eq 7 and 8. The values of the back-reaction rate constant k_{21} are further

---

(9) Sutin, N. *Prog. Inorg. Chem.* **1983**, *30*, 441.

revealed by this analysis to be quite large, and in consideration of eq 9, back-reaction rates of this magnitude indeed lead to a substantial depression of the net forward reaction rate.

The preceding analysis indicates that the rates of electron transfers between metal complexes contacting one another at a polymer–polymer interface, once the back-reaction rate effect is included, can be accounted for with remarkably simple electron-transfer theory. We must caution, however, that the agreement seen in Table I is not exact; the uncertainties in the experimental k_{12} and k_{21} measurements are considerable and in the case of reaction 1, k_{12} and $k_{12(TH)}$ differ by a factor of 2.

In the face of these experimental uncertainties it is important to point to the caveats and limitations of the experiment–theory comparison. First, kinetic results are rarely exact enough to confirm a physical model in a precise sense, and in the present case the experimental/theory comparison is insufficiently exact to assert that the interfaces concerned are perfectly defined. That is, the comparison leaves room for some undetected imperfection (perhaps as much as a factor of 2×) in the contacts between the layers of poly[$Os(bpy)_2(vpy)_2]^{2+}$ and poly[$Ru(vbpy)_3]^{3+}$ sites at both polymer/polymer and polymer/Pt interfaces. Likewise we cannot exclude the possibility that a monolayer or two of the sites at the polymer/polymer interface might not intermingle, or that small, undetectable differences might exist in the barriers to electron transfers at polymer/polymer and polymer/Pt interfaces. Second, there is a real possibility of compensating effects, where over-estimation of the back-reaction rate (due to our assumption of eq 10) becomes balanced by either voids in the polymer/polymer interface contact region or larger electron-transfer barriers associated with the interfacial region. We have no way to evaluate this possibility and can conclude only that such effects must be a good deal smaller than the 50–70-fold difference which would correspond to (eq 6) neglect of the back-reaction rate altogether.

Finally, we should note that Z was assumed as 10^{11} M^{-1} s^{-1} in the calculation of $k_{12(TH)}$ (Table I), and similar values emerged (see Table I footnote) from the fitting of eq 9–11 to the experimental results. That a value of collision frequency should be near that of the usual liquid solvent diffusion-controlled would not be immediately anticipated. It in one sense implies that the interfacial region for solvent-wetted polymer is in fact rather fluid, i.e., that on a microscopic level (one metal complex diameter dimension) the poly[$Os(bpy)_2(vpy)_2]^{2+}$ and poly[$Ru(vbpy)_3]^{3+}$ sites have relatively unimpeded mobility. This microscopic fluidity would be consistent with the near-ideal electron-transfer behavior we have observed for electron self-exchange kinetics within the polymer phase in previous studies.[4] It should also be remembered that these polymers are essentially undiluted metal complexes, and the sites are already at or near contact in their equilibrium positions.

Returning to the result of Figure 4B, this shows how the potential E_{interf} of the Pt metal layer separating the two polymers poly[$Os(bpy)_2(vpy)_2]^{2+}$ and poly[$Ru(vbpy)_3]^{2+}$ varies with E_{scan}. This is a novel measurement of the interface between two chemically reacting solids. The potential E_{interf} of the Pt layer "floats" and reflects the oxidation states of the polymer layers which contact it. Ignore the effects below 0.5 V for now. Figure 4B shows that between E_{scan} = 0.5 and 0.94 V, as E_{scan} is made more positive and the poly[$Os(bpy)_2(vpy)_2]^{2+}$ film is converted to the Os(III) state, E_{interf} is equal to E_{scan}. This demonstrates that the entire poly[$Os(bpy)_2(vpy)_2]^{2+/3+}$ film remains in thermodynamic equilibrium with the controlling electrode potential (E_{scan}). That is, the concentration ratio of Os(II) and Os(III) sites is the same on both sides of the polymer film; on the Pt layer side the electrode senses the Os(II)/Os(III) ratio and assumes the corresponding Nernstian potential. This result is one justification for the use of eq 10 (vide supra).

As E_{scan} in Figure 4B enters the potential region where reaction 2 begins to occur, as evidenced by currents observed at the E_{fixed} electrode (Figure 4A, dashed line), the interfacial potential E_{interf} levels off and becomes constant. It is significant that this limiting value of E_{interf} is identical with the half-maximum current of the interfacial wave. In Figure 4, this is 0.945 V vs SSCE. It is further significant that this potential is the same as the average of the two formal potentials of the redox couples of the polymer pair, 0.94 V. This phenomenon, of $E_{interf} = E_{1/2} = \text{av } E^{\circ\prime}$, was also observed in analogous experiments with the Pt layer–separated polymer pair used for reaction 3 and so seems to be a general effect.

We interpret E_{interf} as a *mixed potential.*[10] In metal corrosion chemistry, it is known that the potential of a slowly corroding (being oxidized) metal is related to a combination of the formal potentials of the metal/metal ion and the oxidant redox couples. This "mixed potential" represents a dis-equilibrium state, since the two couples are reacting and electrons are being transferred from one couple to the other via the metal phase. The situation is entirely analogous to that in Figures 3 and 4, where two polymer phase redox couples are slowly reacting with one another via the intervening Pt metal layer phase (whose potential E_{interf} we measure). Mixed potential theory furthermore predicts[11] that if the transport rates and concentrations of the reactants are equal, then $E_{mixed} = (E_1^\circ + E_2^\circ)/2$. The electron-diffusion rates and metal complex site concentrations of the polymer films employed in reactions 2 and 3 are expected to be quite similar, so the mixed potential theory provides an explanation of why $E_{interf} = (E_{Os}^\circ + E_{Ru}^\circ)/2$.

Finally, at potentials more negative than 0.5 V in Figure 4B, the potentials on the opposite sides of the poly[$Os(bpy)_2(vpy)_2]^{2+}$ film are clearly not in equilibrium with one another on the experimental time scales employed. The potentials are not equal to one another, and there is hysteresis between forward and reverse potential scans. This dis-equilibrium is an expected consequence of electron transport by eq 5, by which transport is expected to be slow if the film has no significant mixed valency.

Acknowledgment. This research was supported in part by grants from the National Science Foundation and the Office of Naval Research. The authors acknowledge useful discussion with Professor R. P. Buck of UNC.

---

[10] Delahay, P. *Double Layer and Electrode Kinetics*; Interscience Publishers: New York, 1965; p 172.

[11] Wagner, C.; Traud, W. *Z. Elektrochem.* **1938**, *56*, 391.